PAPER REF: 19907

DEVELOPMENT OF DISINTEGRATED HYBRID CROSS LAMINATED TIMBER

Lucas Bienert[1](*), Nils Schumacher[1,2], Stefan Winter[1], Klaus Richter[2]

[1]Chair of Timber Structures and Building Construction, Technical University of Munich, Germany
[2]Chair of Wood Science, Technical University of Munich, Germany
(*)*Email:* lucas.bienert@tum.de

ABSTRACT

The shift within the building industry towards more sustainable constructions leads to a rising demand for wood as a building material – mainly softwood species like spruce – to replace the energy and carbon intensive materials steel and concrete. While today, the European forests still produce enough wood in the required quality, in the future the forests will come under increasing pressure due to climate change and the rising demand. To deal with this challenge, new engineered wood products must be developed that use native, climate change resistant hardwood species like beech instead of the more vulnerable softwood species like spruce. At the same time, the overall demand for wood must be limited by raising the material efficiency. One new product that addresses both issues is disintegrated hybrid cross laminated timber (DH CLT), which is presently being developed at the TU Munich. In this work, different lay-ups of DH CLT are investigated by means of mechanical experiments, complemented by numerical analyses using the Finite Element (FE) method and analytical calculations.

Keywords: cross laminated timber, CLT, disintegrated, hybrid, wood products, hardwood.

INTRODUCTION

The basis for the new product development is conventional cross laminated timber (CLT). It is today widely used in timber constructions, particularly in multi-storey buildings like offices and residential buildings. CLT generally consists of an odd number of layers of boards where every second layer is rotated by 90°. The individual layers are then glued together. Thus, a two-dimensional engineered wood product for ceiling plates and walls is produced. Its advantages include a very good dimensional stability and the possibility to create plates that can transfer loads in both directions. However, CLT uses great amounts of material, especially the inner layers contribute only little to the overall load bearing capacity for bending. That is why CLT is a very suitable product for advancements in material efficiency.

To reach this goal, as a first step, hardwood is incorporated into the CLT, creating so-called hybrid CLT. Hardwood is a material that is only used little for construction purposes today, especially beech is actually mostly used as a thermal energy resource, i.e. as fire wood, so that the carbon that is stored inside the wood is instantly emitted again. Moreover, within the research project of the TU Munich, it is intended not to use up newly logged hardwood but to use waste wood from the timber industry which still has an acceptable quality.

As a second step, individual boards are removed from the inner layers of the hybrid CLT. This is possible because hardwood – even the waste wood – has significantly higher stiffness and strength properties compared to softwood (cf. Hunger & Van de Kuilen 2015). The end product is then called disintegrated hybrid CLT, an example is presented in Figure 1. Next to the higher

material efficiency, the gaps in between the boards can e.g. be used to integrate prestressed tendons, vibration dampers or insulation.
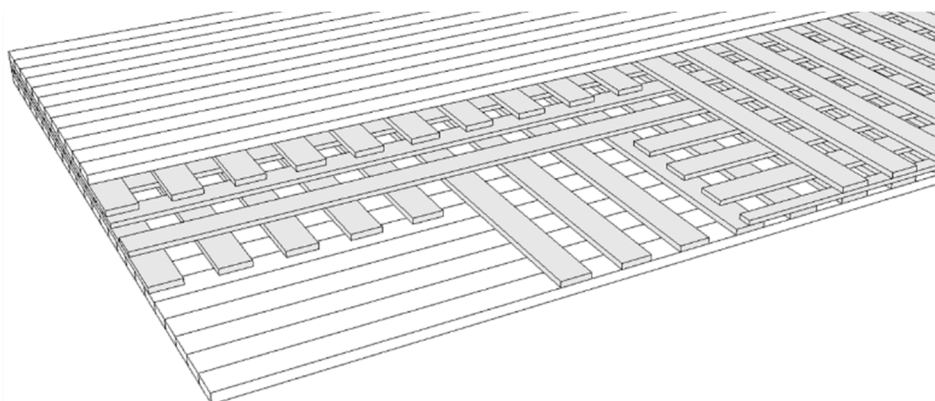

Fig. 1 – View into a disintegrated hybrid CLT element (white = softwood, grey = hardwood).

For all investigations, a standard lay-up consisting of five layers is used, where the two cross layers and the middle layer can be made of beech and disintegrated. The remaining layers are made of spruce. To quantify the degree of disintegration, the following definitions are made:

cross layer density: $$d_c = b_c/(b_c + e_c)$$ (1)

middle layer density: $$d_m = b_m/(b_m + e_m)$$ (2)

where:
d_c, d_m [-] cross layer and middle layer density
b_c, b_m [mm] width of an individual board in the cross layer or middle layer
e_c, e_m [mm] spacing between the boards in the cross layer or middle layer

MATERIAL

The timber material in the test specimens is spruce (*Picea abies*) and beech (*Fagus sylvatica*). The spruce is used for the outer layers and is graded in the strength class C24 or better. The beech lamellae are for the inner layers. They can have a lower quality, because of the negligible contribution of the inner layers to the overall load bearing capacity for bending. In order to obtain the planned lower quality grades, it is necessary to understand the cross-section of the beech log and the cutting method. The green marked area (Figure 2) shows the part of the cross section that is around the pith.
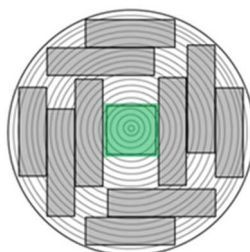

Fig. 2 - Typical method for cutting beech (green = area
in the cross section of low quality sawn timber).

According to DIN 4074-5, the German standard for strength grading of hardwood, lamellae with pith are not permitted for compliance with the grading criteria. However, the experimental

investigations on the bending shear specimens showed the great potential and high strength and stiffness of the used beech lamellae under rolling shear loading. This potential even makes it possible to disintegrate the lamellae. These positive properties and the fact of upgrading low quality timber and keeping it in the material cycle would be lost if it were not used.

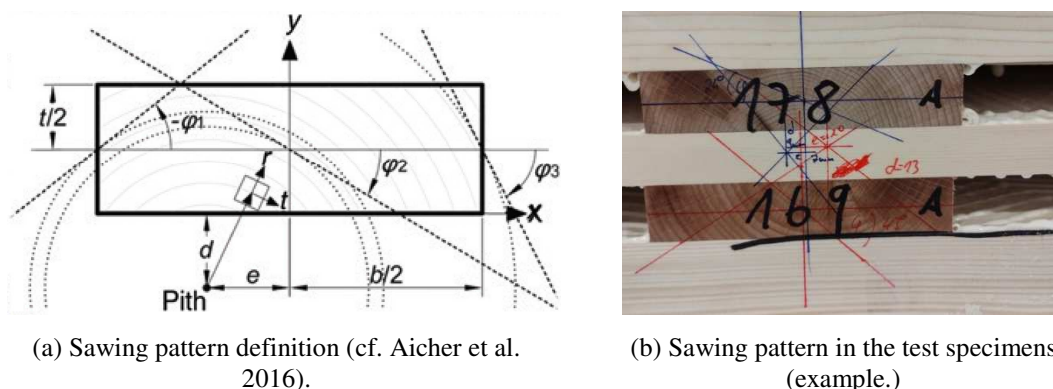| (a) Sawing pattern definition (cf. Aicher et al. 2016). | (b) Sawing pattern in the test specimens (example.) |

Fig. 3 – Sawing patterns, definition and application in the test specimens.

For the investigations, a total of 108 lamellae were examined in the area of the supports of the test specimens. Two sawing patterns were recorded for every lamella, one at each end face, also because the course of the mark varies greatly over the length of the lamella, Figure 3. This means that 216 sectional views were taken. 4 sawing patterns could not be assigned without doubt and are therefore not considered.

Table 1 – Evaluation of the sawing pattern examinations.

	all	including pith	without pith	failed (total)	failed including pith	failed without pith
n (-)	212	35	177	17	10	7

Table 1 shows that 8% of all the examined sawing patterns failed during the test. From the sawing patterns including pith 29% failed but only 4% of the sawing patterns without pith failed.

A strong influence of the pith on the rolling shear strength can be seen. The examination of the sawing patterns on the supports of the test specimens could confirm the results of the mechanical rolling shear investigations by Aicher et al. (2016) in their tendency, cf. Table 2.

Table 2 – Strength results depending on sawing pattern of the investigated specimens (cf. Aicher et al. 2016).

Rolling shear strength $f_{v,r}$ (N mm^{-2})	all	including pith	without pith
n (-)	45	13	31
Mean	5,5	4,5	6,0
SD	1,2	1,1	0,9
COV	22%	26%	16%
X_{05}	3,3	2,1	4,5

MECHANICAL EXPERIMENTS

Several specimens with different cross layer and middle layer densities using the described materials were developed and tested first in a four-point bending shear test with a ratio of span to height of the cross-section of $L/h = 12$ and then in a similar bending test with a ratio of span to height of $L/h = 26$. The purpose of the relatively short span for the bending shear tests was to provoke a shear failure at one of the two supports. The hypothesis was that shear failure will be decisive for the disintegrated elements because the middle layers mainly contribute to the shear resistance of a cross-section. The aim was to determine the shear strength for different failure modes of the different variants and to calculate the shear stiffnesses.

The bending tests on the other hand are more suited to determine the bending stiffness. Concerning the strength of the different variants, it was expected to see similar maximum loads, since the bending strength is governed by the outer layers which are always the same for all variants. It would, however, be interesting to see if for some lay-ups the shear failure will still be decisive over bending failure.

The setup for both types of bending tests is shown in Figure 4 and Table 3, they only differ in the length l_2 between support and load.
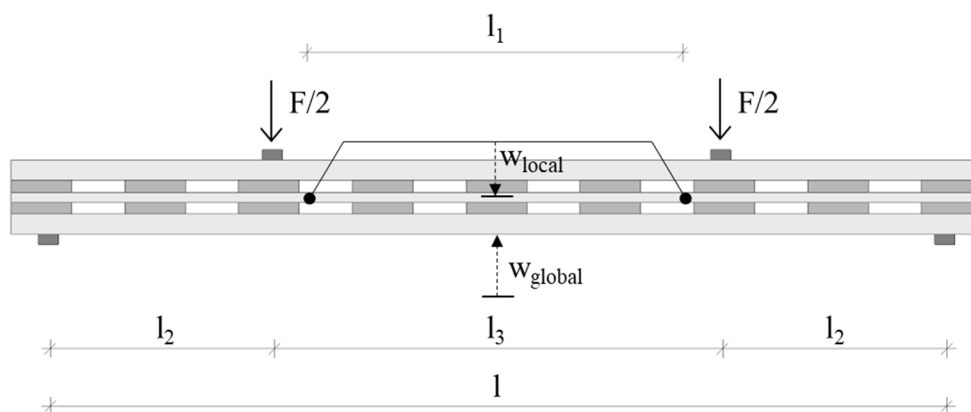

Fig. 4 – Setup for the bending shear and bending tests.

Table 3 – Geometrical data for the test setup of the bending shear and bending tests.

	l_1	l_2	l_3	l
bending shear tests	740 mm	444 mm	888 mm	1776 mm
bending tests	740 mm	1482 mm	888 mm	3852 mm

Next to the disintegrated specimens (B-1 to B-7), conventional CLT-specimens entirely made of spruce (S-0) as well as hybrid CLT-specimens without disintegration (B-0) were tested as a reference. The results are shown in the next two figures, where Figure 5 displays the maximum load from the bending shear tests and Figure 6 displays the effective bending stiffnesses (from the bending tests) and the shear stiffnesses (from the bending shear tests). While the bending shear tests were carried out with all the presented variants, the bending tests were only conducted with a selection of the most relevant lay-ups. Unfortunately, because technical

problems occurred during the gluing process while manufacturing the bending test specimens, their load bearing capacity was impaired and could not be evaluated.
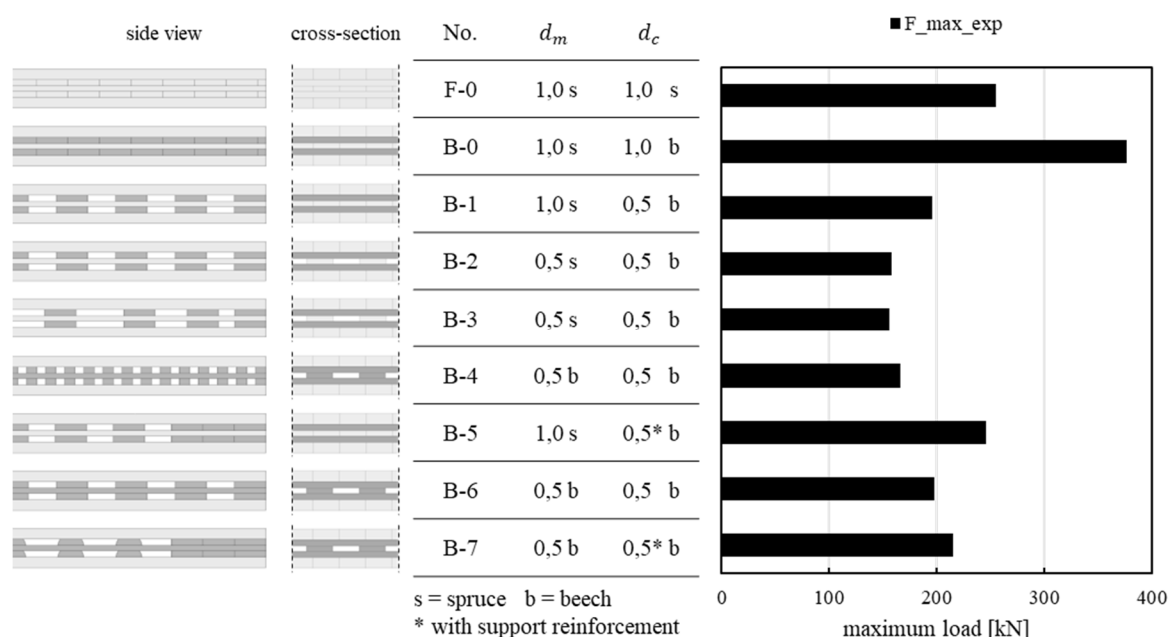

Fig. 5 – Results from the bending shear tests: maximum loads (light grey = spruce, dark grey = beech).
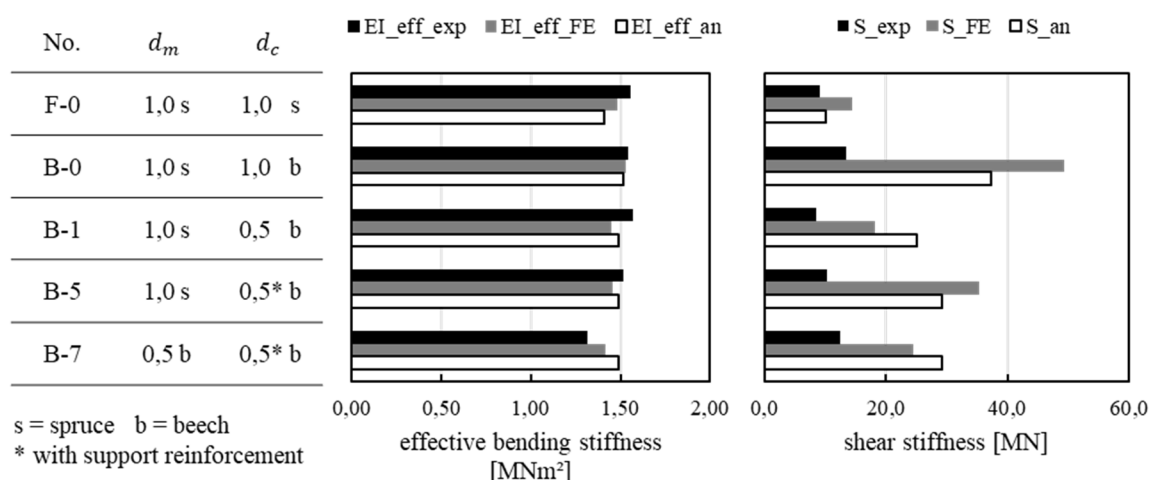

Fig. 6 – Results from the bending shear and bending tests (_exp) in comparison to FE (_FE) and analytical (_an) calculations: stiffnesses.

The results of the maximum loads show that, even though beech has more than twice the rolling shear strength of spruce (cf. Aicher et al. 2016), it was not possible to fully compensate the material reduction. While the spruce reference specimens S-0 reached a mean load of $254\ kN$, the specimens where only the cross layers were made of beech and disintegrated – B-1 with a density of $d_c = 0,54$ – reached only $195\ kN$.

The hybrid CLT specimens without disintegration B-0 reached the highest loads ($377\ kN$). Comparison to the disintegrated variant B-1 shows that there is obviously no linear relationship between the layer density and the capacity of the specimen, because $0,54 \cdot 377 = 204\ kN$ is

still higher than what the disintegrated specimens actually achieved. It can be noted that the ratio of width to height of the cross layer boards seems to have an influence, because B-4 with a similar density of $d_c = 0{,}51$ but much more narrow boards has an even lower maximum load of $166\ kN$. A hint to why this discrepancy occurs is the observed failure of most disintegrated specimens which is characterized by a "rolling off" of whole boards in the cross layers, cf. Figure 7(c).

(a) S-0 Spruce reference: rolling shear failure

(b) B-0 Hybrid CLT reference: longitudinal shear failure

(c) B-4: "Rolling off" of whole boards in the cross layers

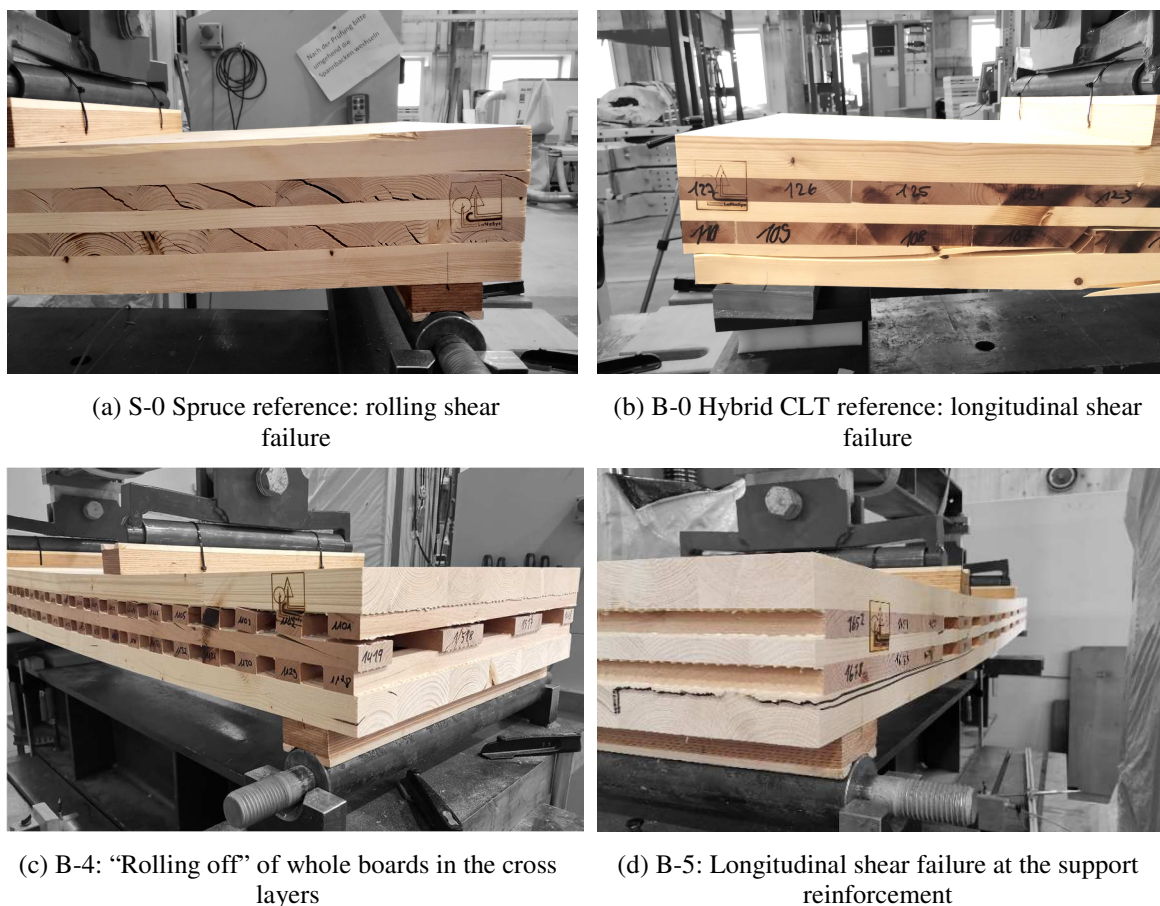(d) B-5: Longitudinal shear failure at the support reinforcement

Fig. 7 – Failure modes of bending shear test specimens.

A rolling shear failure of the beech cross layer boards themselves did not really occur, only a few individual boards failed in that way (8% of the sawing patterns examinations, cf. Table 1), but the overall failure mode was characterised by a combination of shear and tension perpendicular to the grain in the longitudinal layers. The only exceptions were the reference specimens: the spruce reference S-0 failed due to rolling shear in the spruce cross layers (Figure 7 (a)), and the hybrid beech reference B-0 failed due to shear in the longitudinal spruce layers (Figure 7(b)). The latter shows clearly that the rolling shear strength of the beech boards is higher than the longitudinal shear strength of the spruce.

To improve the load bearing behaviour of the elements, two possibilities were investigated: a non-uniform distribution of the cross layer boards, continuously reducing the spacing between the boards towards the supports (B-3), and a support reinforcement, which means that close to the supports, the cross layer boards were arranged completely without gaps and only the middle of the span was disintegrated (B-5 and B-7).

While the non-uniform distribution did not show any significant improvements – especially taking into account the considerably higher production effort –, with the support reinforcements it was possible to increase the capacity of the specimens to $246\ kN$, which is almost the same capacity as the spruce reference specimens S-0. It seems possible that by lengthening the reinforcement further into the middle of the element, the load bearing capacity could be increased even further and also surpass the reference.

Whereas the maximum loads of the different lay-ups vary a lot, the bending stiffnesses are similar, cf. Figure 6. This fact is especially interesting because generally, the stiffness is decisive for CLT elements in buildings, not the load bearing capacity. The effective bending stiffness is calculated from the local deformation measurement inside the shear free part of the span according to formula (3).

$$EI_{eff} = \frac{l_2 \cdot l_1^2}{16} \cdot \frac{\Delta F}{\Delta w_{local}}$$

(3)

The global deformation measurement on the other hand gives the apparent bending stiffness, which additionally includes the effects from the shear deformation in the outer parts of the span, cf. formula (4).

$$EI_{app} = \frac{3 \cdot l_2 \cdot l^2}{48} \cdot \frac{\Delta F}{\Delta w_{global}}$$

(4)

From the difference between the effective and the apparent bending stiffness, the shear stiffness can be calculated:

$$S = \frac{24 \cdot EI_{eff} \cdot EI_{app}}{(3l^2 - 4l_2^2) \cdot \left(EI_{eff} - EI_{app}\right)}$$

(5)

The FE simulations and the analytical calculations give similar results as the experiments, the maximum deviation is 13 % for B-7. This seems not to be a big inaccuracy when taking into account the considerable natural variations of the mechanical properties of wood. For the shear stiffness, however, the deviations are much higher. While the spruce reference can still be modelled fairly accurately both with FE and analytical calculations, the deviations become significant for all the hybrid variants. Both overestimate the shear stiffness, which can be due to incorrect estimates for the material properties of the beech wood itself or mechanical effects not yet considered in the models. Still, qualitatively, the results are already consistent; S-0 has the lowest shear stiffness, B-0 has the highest shear stiffness and the three other variants B-1, B-5 and B-7 have rising shear stiffnesses. Moreover, it has to be noted that the shear deformation usually only has a small influence on the overall deformation and is therefore often completely neglected. In the following, both the FE investigations and the analytical approaches will be described in more detail.

## FINITE ELEMENT INVESTIGATIONS

Numerical investigations using the FE method were carried out with digital twins of all specimens, looking at the internal stress distributions, the direction of the primary stresses, and more. It could be seen clearly that stress concentrations occur at the corners of the cross layer boards for the normal stresses perpendicular to the grain as well as other stresses like the shear stresses or the normal stresses in longitudinal direction, depending on the lay-up, cf. Figure 8.

This could explain the reduction of the load bearing capacity despite the higher strengths of beech. It also correlates with the mentioned observations during the experiments. The initial cracks always started at those corners where the FE model showed stress concentrations, finally leading to the rolling off of the boards.

Because the stress concentrations represent singularities (points of theoretically infinite stress) it is not possible to directly calculate load-bearing capacities of the specimens to compare to the measured test results. It is, however, possible to calculate stiffnesses by measuring the deformations and the same points as for the real specimens and calculating the stiffnesses in the same way.
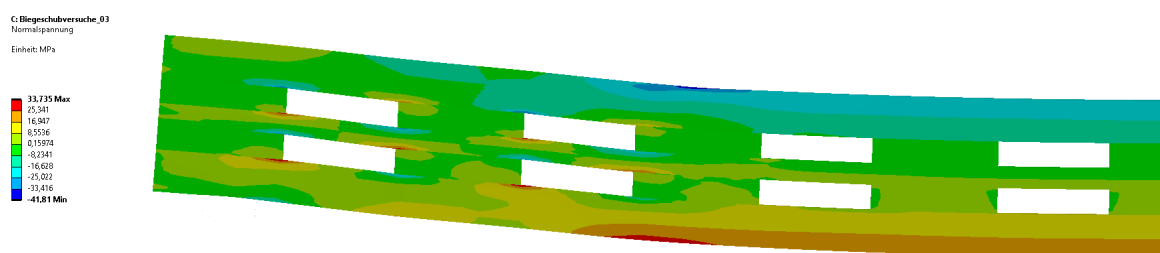
(a) Normal stresses in longitudinal direction
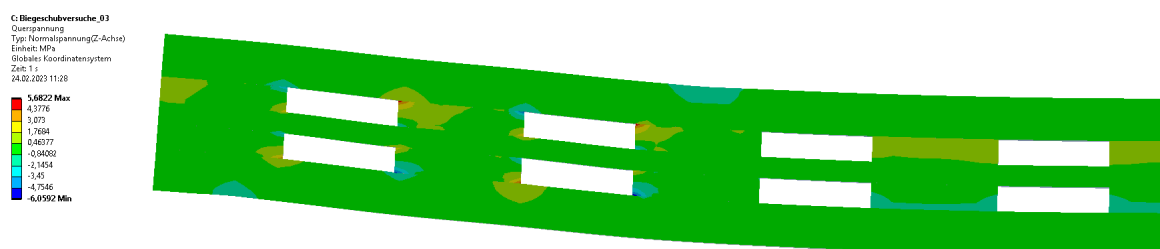
(b) Normal stresses perpendicular to the grain

Fig. 8 – Stress distributions of the digital twin of specimen B-3 (only half the specimen is modelled, deformation is not to scale).

ANALYTICAL CALCULATIONS

As with the FE investigations, it proved to be a challenge to derive strength vaues purely from mechanical considerations because of the stress concentrations and interactions at the corners of the cross layer boards. The approach that was eventually chosen was to determine an effective rolling shear strength of a cross layer from the experimental results of the bending shear tests. Thus, it was possible to give an effective rolling shear strength for each lay-up that can be used to determine the shear load bearing capacity of a plate with the corresponding lay-up. The bending load bearing capacity in turn can be calculated as for usual CLT because the inner layers have almost no influence on the bending strength. The smaller of the two values determines the failure mode and the overall load bearing capacity.

The effective rolling shear strength can be calculated as follows:

$$f_{r,eff} = \frac{F_{max}/2 \cdot ES}{EI_{eff} \cdot b} \tag{5}$$

where: ES [MNm]   static moment of area of the outer layer, weighted with the corresponding Young's modulus for spruce

It is important to note that the effective rolling shear strength does not necessarily mean only rolling shear failure is considered – rather it includes all possible failure modes and the influences from the stress concentrations.

Additionally, from the two variants with support reinforcement an effective shear strength for the support reinforcement could be calculated, to make it possible to determine the load bearing capacity of a plate with a certain lay-up and a support reinforcement of arbitrary length. Because the specimens with support reinforcement showed a shear failure in the longitudinal layers (cf. Figure 7(d)), this horizontal shear stress was calculated from the maximum loads of the experiments, using formulae 6 to 8.

The force resulting from the horizontal shear stress in the adhesive joint between the bottom layer and the cross layer must be in equilibrium with the tensile force T from the bending stresses σ in the bottom layer.

$$\sigma = \frac{E \cdot M_{max}}{EI_{eff}} \cdot z \tag{6}$$

where: E Young's modulus of the bottom layer for spruce

       $M_{max} = F_{max}/2 \cdot l_2$ maximum bending moment

       z distance from the neutral axis to the centre of the bottom layer

$$T = \sigma \cdot t \cdot b \tag{7}$$

where: t thickness of the bottom layer

       b width of the specimen

The effective shear strength of the support reinforcement can then easily be calculated assuming a constant distribution of the horizontal shear stress along the reinforcement.

$$f_{v,eff}^* = \frac{T}{b \cdot l^*} \tag{8}$$

where: l^* length of the support reinforcement

The results are presented in Table 4.

As expected, the hybrid reference B-0 has the highest effective rolling shear strength, and the disintegrated variants show lesser values. B-6 and B-7 with beech also in the middle layer have the highest strength of all disintegrated variants, although none reaches the spruce reference S-0. The effective shear strength of the support reinforcement, however, is higher, so that in combination, the strength of the spruce reference can be exceeded.

Table 4 – Effective strengths of the different lay-ups from the results of the bending shear tests.

No.	effective rolling shear strength of the lay-up $f_{r,eff}$ [N/mm²]	effective shear strength of the support reinforcement $f^*_{v,eff}$ [N/mm²]
S-0	2,05	-
B-0	2,77	-
B-1	1,63	-
B-2	1,49	-
B-3	1,66	-
B-4	1,46	-
B-5 *	1,46 [1]	2,29
B-6	1,79	-
B-7 *	1,79 [1]	2,62

* with support reinforcement

[1] For the variants B-5 and B-7 with support reinforcement, no individual effective rolling shear strength was calculated. Because – apart from the reinforcement – the variants have the same lay-up as the variants B-4 and B-6, respectively, the same effective rolling shear strength values are assumed.

The effective bending stiffnesses were calculated using the γ-method according to formula (9), which is also described in EN 1995-1-1. The method has to be adapted for CLT, with the cross layers representing the mechanical connection of the longitudinal parts of the cross-section.

$$EI_{eff} = \sum_{i=1,3,5} E_i \cdot I_i + \gamma_i \cdot E_i \cdot A_i \cdot a_i^2 \qquad (9)$$

The γ-factor, which represents the efficiency of the connection of the longitudinal layers by the cross layers, can be calculated according to formula (10).

$$\gamma_i = \frac{1}{1 + \dfrac{\pi^2 \cdot E_i \cdot t_i}{l^2 \cdot d_c \cdot G_{i \pm 1}/t_{i \pm 1}}} \qquad (10)$$

where: i [-]   layer number, only applicable to the outer layers 1 and 5 ($\gamma_3 = 1,0$)

          $t_i, t_{i\pm1}$ [mm]   thickness of an outer layer and the respective cross layer on the inside of the considered outer layer

          $G_{i\pm1}$ [N/mm²]   rolling shear modulus of the respective cross layer

One has to bear in mind, however, that the γ-method is actually only applicable to simply supported beams with a sine-shaped distribution of the bending moment, which is not the case for the described four-point bending tests. Still, for the trapezoidal distribution of the bending moment it can be used as a good approximation.

The shear stiffnesses were calculated using formula (11).

$$S = \kappa \cdot GA = \kappa \sum G_i \cdot A_i \tag{11}$$

where: κ [-]   shear correction factor

The shear correction factor can be calculated as follows, based on Wallner-Novak et al. (2013).

$$\kappa = \frac{GA}{EI^2} \cdot \int_h \frac{ES^2}{G \cdot b} dz \tag{12}$$

With the static moment of area, weighted with the corresponding Young's moduli for each layer:

$$ES = \int_z^{z_{max}} E \cdot z \cdot dA \tag{13}$$

DISCUSSION

The overall goal of this research is to develop a hybrid disintegrated lay-up that is equal to conventional spruce CLT. This, however, does not necessarily mean that all properties – shear capacity, bending capacity, stiffness and so on – must be equal to the conventional CLT. Rather, it is important to optimise the lay-up so that each property is just good enough and as much material as possible can be reduced. E.g. for a standard CLT floor plate in a domestic building, generally the deflection and vibration become decisive, while the bending capacity is only utilised to a relatively small degree. This means that the bending capacity could well be reduced by a certain disintegrated lay-up without reducing the overall performance of the element.

Although some of the presented variants already reach similar load bearing capacities as conventional CLT, the other variants may also have a value, especially because the bending

stiffness is decreased negligibly. Variants with very small lamellae like B-4 have the advantage that it is possible to use an even bigger part of the log than with bigger lamellae (cf. Figure 2).

By carrying out further tests to verify and improve the analytical approaches, calculation methods shall be worked out that allow an optimised design of disintegrated hybrid CLT. Already, the results show that it is possible to design DH CLT plates that can replace conventional CLT or even extend the possible uses towards higher spans.

REFERENCES

[1] Aicher S, Zachary C, Hirsch M, Rolling shear modulus and strength of beech wood laminations. Holzforschung, 2016, 70(8), pp.773-781.

[2] EN 1995-1-1:2010: Eurocode 5 – Design of timber structures – Part 1-1: General rules and rules for buildings, 2010.

[3] Hunger F, Van de Kuilen J-W, Festigkeitsprofile von heimischen Laubhölzern. Final report for the project 13508 / X40. Holzforschung München, 2015.

[4] Wallner-Novak M, Koppelhuber J, Pock K, Brettsperrholz Bemessung. Grundlagen für Statik und Konstruktion nach Eurocode. ProHolz Austria, 2013.